Room-Temperature Characterization of a Mixed-Valent μ-Hydroxodicopper(II,III) Complex

James A Isaac, Franc A Gennarini, Isidoro López, Aurore Thibon-Pourret, Rolf David, Gisèle Gellon, Beátrice Gennaro, Christian Philouze, Franc Meyer, Serhiy Demeshko, et al.

Inorganic Chemistry

Communication

pubs.acs.org/IC

Room-Temperature Characterization of a Mixed-Valent μ-Hydroxodicopper(II,III) Complex

James A. Isaac,[†] Federica Gennarini,[‡] Isidoro López,[‡] Aurore Thibon-Pourret,[†,§] Rolf David,[†] Gisèle Gellon,[†] Béatrice Gennaro,[†] Christian Philouze,[†] Franc Meyer,[∥] Serhiy Demeshko,[∥] Yves Le Mest,[‡] Marius Réglier,[⊥] Hélène Jamet,[†] Nicolas Le Poul,*[,‡] and Catherine Belle*[,†]

[†]DCM (UMR CNRS 5250), Université Grenoble-Alpes, CS 40700, 38058 Grenoble, France

[‡]CEMCA (UMR CNRS 6521), Université de Bretagne Occidentale, 6 avenue Le Gorgeu, 29238 Brest, France

[§]Institut de Chimie, CLAC, UMR 7177 CNRS, Université de Strasbourg, 67008 Strasbourg, France

[∥]Institut für Anorganische Chemie, Georg-August Universität Göttingen, Tammannstraße 4, 37077 Göttingen, Germany

[⊥]Aix-Marseille, CNRS, Centrale Marseille, ISM2 UMR 7313, 13397 Marseille, France

Supporting Information

ABSTRACT: Bis(μ-hydroxo)dicopper(II,II) bearing a naphthyridine-based ligand has been synthesized and characterized in the solid state and solution. Cyclic voltammetry at room temperature displays a reversible redox system that corresponds to the monoelectronic oxidation of the complex. Spectroscopic and time-resolved spectroelectrochemical data coupled to theoretical results support the formation of a charge-localized mixed-valent $Cu^{II,III}_2$ species.

In past decades, significant progress has been achieved in the field of Cu/O_2 chemistry relevant to metalloenzymes capable of oxidizing substrates.[1,2] Numerous biomimetic dicopper complexes have provided structural and spectroscopic data about Cu_2/O_2 species involved in such processes.[3−8] Interestingly, theoretical studies have postulated that a mixed-valent $Cu^{II,III}_2/O_2$ cluster in the active site could be the oxidizing intermediate in the catalytic cycle in the particulate methane monooxygenase (pMMO) enzyme.[9−11] So far, only one example of such a $Cu^{II,III}_2$ species has been characterized by spectroscopic means at low temperatures.[12]

In the present work, we have prepared and characterized a mixed-valent $Cu^{II,III}_2$ species that is stable for several seconds at room temperature (RT) in CH_3CN. The chosen ligand [DPMN = 2,7-bis(dipyridyl)methyl-1−8-naphthyridine] displays interesting properties,[13,14] such as (i) two well-defined coordination sites with a short metal−metal distance and (ii) a redox-innocent bridging spacer. In this context, a new bis(μ-hydroxo)dicopper(II,II) complex, $[Cu^{II}_2(DPMN)(\mu\text{-}OH)_2(OTf)](OTf)$ (**1**·$(OTf)_2$, where $OTf^- = CF_3SO_3^-$), was synthesized from a reaction in tetrahydrofuran between the DPMN ligand, $Cu(OTf)_2$, triethylamine, and water (details in the Supporting Information, SI). Crystals suitable for X-ray diffraction (XRD) were obtained from the resulting powder by vapor diffusion of diisopropyl ether into CH_3CN. The unit cell contains two independent $[Cu^{II}_2(DPMN)(\mu\text{-}OH)_2(OTf)](OTf)\cdot 1.8CH_3CN$ entities, **1A**·$(OTf)_2$ and **1B**·$(OTf)_2$. Both show no significant differences in their bond distances and angles (see the SI). The cationic unit of **1A**·$(OTf)_2$ is shown in Figure 1. Each unit consists of two Cu atoms bridged by two hydroxo moieties with Cu1−OH−Cu2 angles in the range of 90.11−90.67°.

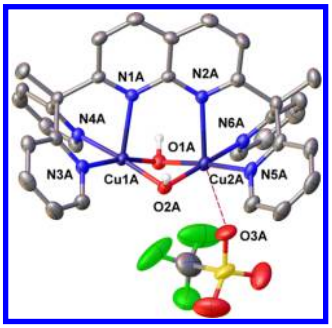

Figure 1. Molecular structure of the cationic part of **1A**·$(OTf)_2$ determined by XRD with thermal ellipsoids set at 50%. H atoms (except from the OH) were omitted for clarity. Selected bond and distances are given in the SI.

The Cu1···Cu2 bond distance (~2.75 Å) is one of the shortest reported for bis(μ-hydroxo)dicopper(II) complexes bridged by a spacer[15−17] and close to the ~2.6 Å value observed in the dinuclear site of pMMO.[11,18] The coordination polyhedron around the Cu1A atom is a distorted square pyramid whose apical position is occupied by the naphthyridine N1A atom at 2.276 Å. Because of the presence of a triflate anion at the Cu2A site, the two Cu atoms are not in identical coordination environments. Cu2A is found in a distorted octahedral geometry with axial positions occupied by the N2A atom at an elongated distance of 2.353 Å compared to 2.276 Å for Cu1−N1A and the O3A atom from a triflate at 2.615 Å. The temperature-dependent magnetic susceptibility for **1**·$(OTf)_2$ was measured at 5000 Oe from 295 to 2 K. The $\chi_M T$ versus T curve for the dinuclear complex (Figure S2) was simulated by using the isotropic exchange Hamiltonian $\hat{H} = -2J\hat{S}_1\hat{S}_2$. The exchange coupling constant, $J = +113$ cm^{-1}, is large and positive, indicating the presence of strong ferromagnetic interactions between the two

Received: June 23, 2016
Published: August 12, 2016

DOI: 10.1021/acs.inorgchem.6b01504
Inorg. Chem. 2016, 55, 8263−8266

Cu^{II} ($S = {}^1/_2$) ions within the dinuclear complex, in accordance with the acute Cu−O(H)−Cu angles (see the SI) and previous studies on μ-OH $Cu^{II,II}{}_2$ complexes.[19,20]

In CD_3CN, the paramagnetic ^1H NMR spectrum displays seven observable signals (7.7−133 ppm range; Figures S3−S5), which are consistent with a more symmetrical structure in solution. On the ^{19}F NMR spectrum (+460 to −140 ppm range), a unique peak at +85 ppm versus C_6F_6 is observed upon dissolution of $\mathbf{1}\cdot(OTf)_2$ in CD_3CN, suggesting that all triflate anions are in the same environment and not coordinated to Cu cations in solution or exchanging rapidly on the NMR time scale (Figure S6). The X-band electron paramagnetic resonance (EPR) spectrum (CH_3CN, 15 K) is silent (Figure 2B). In

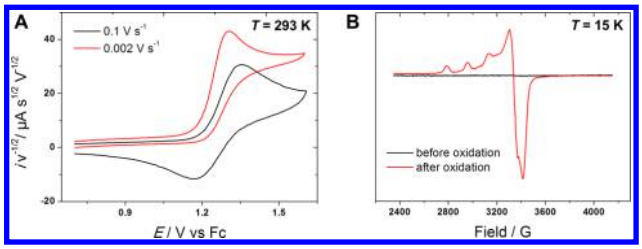

Figure 2. (A) RT scan-rate-normalized cyclic voltammograms (E/V vs Fc^+/Fc) of $\mathbf{1}\cdot(OTf)_2$ (C = 1 mM) in 0.1 M NBu_4PF_6/CH_3CN at ν = 0.002 V s^{-1} (red) and ν = 0.1 V s^{-1} (black). (B) EPR spectra (15 K) of $\mathbf{1}\cdot(OTf)_2$ before (black) and after (red) low-temperature (233 K) bulk electrolysis in NBu_4ClO_4/CH_3CN (ν = 9.419 GHz).

CH_3CN, $\mathbf{1}\cdot(OTf)_2$ exhibits intense electronic transitions (Figure S13) in the UV region similar to the free ligand, and these have been assigned as $\pi-\pi^*$ transitions[14] at 262, 307, 311, and 320 nm. The low-energy band of the d → d transition is observed at 580 nm ($\varepsilon \sim 70$ M^{-1} cm^{-1}). Cyclic voltammetry (CV) of $\mathbf{1}\cdot(OTf)_2$ in NBu_4PF_6/CH_3CN shows an oxidation process that is fully irreversible at low scan rate (ν) but becomes quasi-reversible for $\nu \geq 0.1$ V s^{-1} [E^0 = 1.26 V vs Fc^+/Fc (=1.66 V vs SCE); ΔE_p = 190 mV; Figure 2A]. Plots of the current function ($i/\nu^{1/2}$) against potential E and ν (Figure S8) indicate the occurrence of an ECE mechanism (E = electrochemical and C = chemical), which involves a transient oxidized species having a lifetime of several seconds at T = 293 K (see the SI for further explanations).[21,22] Aiming at calculating the number of electrons (n) involved in the oxidation process, we first performed NMR DOSY experiments (Figure S7) to determine the diffusion coefficient value for $\mathbf{1}\cdot(OTf)_2$ in KPF_6/CH_3CN at 293 K [D = 1.0 (±0.1) 10^{-5} cm^2 s^{-1}]. CV at different scan rates was then used to calculate n by assuming the reversible case for ν > 0.1 V s^{-1}. Indeed, plots of i_{pa} versus $\nu^{1/2}$ yielded n = 1 knowing D, according to the Randles−Sevcik equation (Figure S9).[23] In the same manner, chronoamperometry and rotating-disk electrode voltammetry confirmed the monoelectronic character of the oxidation (Figures S10 and S11 and Table S1). The high value of the oxidation potential determined for $\mathbf{1}\cdot(OTf)_2$ (ca. 1.3 V vs Fc^+/Fc) precludes chemical oxidation.[24] Nevertheless, in order to further investigate the oxidation process, electrochemical and spectroelectrochemical studies were carried out at −40 °C. Decreasing the temperature induced a different redox behavior. Indeed, the system at E = 1.26 V versus Fc^+/Fc became reversible at a low scan rate (ν = 0.01 V s^{-1}; Figure S12) in contrast to the irreversible system at RT. This was accompanied by an increase of the peak-to-peak separation due to a decrease of the electron-transfer kinetics with T. The one-electron-oxidized species was then generated by exhaustive electrolysis of the solution at −40 °C (details in the SI). Noticeably, the pale-purple solution turned to yellow-brown upon oxidation and decomposed into a greenish mixture in less than 1 h. Interestingly, UV−vis and X-band EPR characterization of the transient yellow product was performed and revealed the appearance of an UV−vis absorption band at λ = 424 nm (ε = 1250 M^{-1} cm^{-1}; Figure S13) as well as an axial EPR spectrum with a four-line pattern in $g_{\|}$ from 15 to 200 K (Figures 2B and S16).[25] This indicates hyperfine coupling to only one Cu^{II} consistent with a localized valence similar to the one previously described.[12] The fitting led to the following parameters: $g_{\|}$ = 2.21, $g_{\perp}$ = 2.02, and $A_{\|}$ = 174 × 10^{-4} cm^{-1} (Figure S17), suggesting a square-pyramidal geometry for the Cu^{II} ion. Spectroscopic EPR characterization of the final greenish product showed a broad spectrum, which suggested a mixture of several Cu^{II} complexes in solution (Figure S15).

UV−vis time-resolved spectroelectrochemistry was then carried out for the RT detection of the transient species in a time-resolved manner (thin-layer conditions; one spectrum every 0.5 s). An absorption band was detected at λ = 424 nm upon application of a high potential value (E = 1.6 V) starting from the open-circuit potential (E = 0.8 V; Figure 3). This band

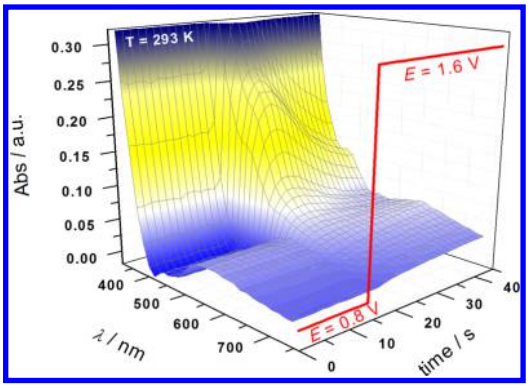

Figure 3. RT time-resolved UV−vis spectrum of $\mathbf{1}\cdot(OTf)_2$ (C = 10 mM; optical path = 0.2 mm) in 0.1 M NBu_4PF_6/CH_3CN upon application of a potential at the working electrode E = 0.8 V versus Fc^+/Fc (first 15 s) and E = 1.6 V (after 15 s).

disappeared progressively within tens of seconds, indicating that the mixed-valent species is relatively stable at RT in agreement with CV at ν = 0.1 V s^{-1}. The same experiment performed at −40 °C led to full stabilization of the monooxidized complex, as shown by UV−vis spectroscopy (Figure S14). In the near-IR (NIR) region, a low-intensity and broad absorption band centered at λ = 1344 nm (ε = 90 M^{-1} cm^{-1}) was detected (Figure S18). This band disappeared and reappeared reversibly by switching between 0.8 and 1.6 V (Figure S19). Fitting of the NIR band allowed the determination of the bandwidth at half-height ($\Delta\tilde{\nu}_{1/2}$ = 2520 cm^{-1}; Figure S20). This gives access to the minimum value for the electronic coupling matrix element H_{ab} assuming a Cu−Cu distance of 2.75 Å.[12] The Γ parameter[26,27] (ratio between the experimental and theoretical values of $\Delta\tilde{\nu}_{1/2}$) was also calculated (see the SI). Values found for H_{ab} = 322 cm^{-1} and Γ = 0.39 are typical of a class II system in the Robin−Day classification, i.e., low delocalization of the charge.[28] Hence, the NIR features of $\mathbf{1}^{3+}$ are slightly different from those obtained for the previously reported mixed-valent $Cu^{II,III}{}_2$ complex.[12] Indeed, the present complex displays lower energy frequency and molar extinction coefficient and higher bandwidth at half-height than the above-mentioned analogue. This suggests a lower delocalization of the charge on the dicopper core for $\mathbf{1}^{3+}$ at 233 K. Further

DOI: 10.1021/acs.inorgchem.6b01504
Inorg. Chem. 2016, 55, 8263−8266

investigations were then carried out by density functional theory (DFT) calculations to gain insight into the electronic structure, redox potential, and UV−vis spectroscopic features of the monooxidized complex.[29] For the redox potential, the absolute value of $\mathbf{1}^{2+}$ was computed and reported relative to the computed value of the Fc^+/Fc redox couple (see the SI).[30] DFT calculations predicted a standard potential equal to 1.36 V versus Fc^+/Fc for sequential one-electron oxidation, in good agreement with the experimental data (E^0 = 1.26 V vs Fc^+/Fc). Figure 4 displays a

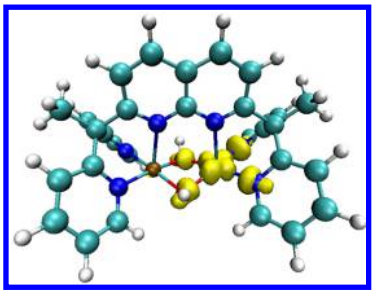

Figure 4. Spin-density plot for $\mathbf{1}^{3+}$ (yellow).

spin-density plot (difference between the α and β densities) for the monooxidized complex. The remaining unpaired electron is mainly localized on only one Cu ion and its adjacent atoms (μ-OH and N_{pyr}). This result confirms the weakly delocalized nature of the mixed-valent $Cu^{II,III}{}_2$ species, in agreement with experimental NIR−vis spectroscopic data. It is also consistent with the EPR results (mono-Cu^{II} signature). The mixed-valent complex also displays Cu−N and Cu−O distances that decrease according to the valence state of the Cu ion. For instance, the Cu−N_{pyr} and Cu−O distances are equal to 1.97 and 2.00 Å for Cu^{II}, respectively, whereas they are significantly lower for Cu^{III} (1.88 and 1.85 Å, respectively). The Cu···Cu distance increases to 2.83 Å for the mixed-valent state species against 2.78 and 2.75 Å for the computed and experimental values, respectively.

Considering the UV−vis spectroscopic features of the monooxidized complex, time-dependent DFT calculations were also performed for $\mathbf{1}^{3+}$ and $\mathbf{1}^{2+}$. Different benchmarks were done to obtain a good description of the absorption band detected experimentally at ∼430 nm. For $\mathbf{1}^{2+}$, there was no band computed at this value (Table S3). The best results were obtained at the wB97XD/IEFPCM level of theory with a transition computed with the lowest-spin contamination of the excited state (S^2 = 0.79 vs 0.75 for a good description of the excited state; Table S2). A band at 1367 nm was also found but with a heavy contamination of spin, which renders this result unreliable. Natural transition orbital analysis[31] provides a reasonable assignment of the band at ∼430 nm as a ligand-to-metal charge transfer essentially between pyridine rings and the Cu^{III} ion (Figure S21). For the monooxidized species, different protonation states of the bridging hydroxo moieties to form a μ-oxo, μ-hydroxo, or a bis(μ-oxo) species were considered. Only $\mathbf{1}^{3+}$ with a bis(μ-hydroxo) core gives different distances between the two Cu and O atoms after geometry optimization (see the description above). For the μ-oxo, μ-hydroxo, and bis(μ-oxo) species, both Cu−O distances stay similar (Table S4), in agreement with a fully delocalized charge ($Cu_2^{2.5}$) of the mixed-valent state. These results, added to the experimental data and the computed redox potential of $\mathbf{1}^{3+}$, seem to indicate that no deprotonation occurs during the oxidation process.

In summary, the use of a bis(tridendate) ligand based on a naphthyridine spacer has provided access to the RT experimental characterization of a mixed-valent μ-hydroxodicopper(II,III) complex with a predominant charge localization on one of the two Cu ions as fully supported by theoretical data. So far, this work displays a rare example of RT spectroscopic and electrochemical identification of such mixed-valent species. The relatively good stability of the mixed-valent complex at RT provides insight for the challenging development of synthetic $Cu^{II,III}{}_2$ models of copper oxygenases such as pMMO. Future work will aim at designing new bioinspired copper complexes with lower oxidation potentials for comparative studies of their reactivity toward C−H activation.

■ ASSOCIATED CONTENT

Supporting Information

The Supporting Information is available free of charge on the ACS Publications website at DOI: 10.1021/acs.inorgchem.6b01504.

Synthesis, electrospray ionization mass spectrometry, magnetism, NMR, electrochemistry, UV−vis, EPR, NIR, and theoretical calculations (PDF)

X-ray crystallographic data in CIF format (CIF)

■ AUTHOR INFORMATION

Corresponding Authors

*E-mail: nicolas.lepoul@univ-brest.fr

*E-mail: catherine.belle@univ-grenoble-alpes.fr

Notes

The authors declare no competing financial interest.

■ ACKNOWLEDGMENTS

Financial support by ANR-13-BSO7-0018 and COST action CM1003 including a STSM grant are acknowledged. This work has been carried out in the frameworks of Labex Arcane (ANR-11-LABX-003) and COST action CM1305 (ECOSTBio). The authors thank C. Calvarin and G. Leroux for the manufacturing of the cryospectroelectrochemical cell and F. Molton for EPR spectra.

■ REFERENCES

(1) Solomon, E. I.; Heppner, D. E.; Johnston, E. M.; Ginsbach, J. W.; Cirera, J.; Qayyum, M.; Kieber-Emmons, M. T.; Kjaergaard, C. H.; Hadt, R. G.; Tian, L. *Chem. Rev.* **2014**, *114*, 3659−3853.

(2) Lee, J. Y.; Karlin, K. D. *Curr. Opin. Chem. Biol.* **2015**, *25*, 184−193.

(3) Mirica, L. M.; Ottenwaelder, X.; Stack, T. D. P. *Chem. Rev.* **2004**, *104*, 1013−1046.

(4) Rolff, M.; Schottenheim, J.; Decker, H.; Tuczek, F. *Chem. Soc. Rev.* **2011**, *40*, 4077−4098.

(5) Citek, C.; Herres-Pawlis, S.; Stack, T. D. *Acc. Chem. Res.* **2015**, *48*, 2424−2433.

(6) Dalle, K. E.; Gruene, T.; Dechert, S.; Demeshko, S.; Meyer, F. *J. Am. Chem. Soc.* **2014**, *136*, 7428−7434.

(7) Kindermann, N.; Bill, E.; Dechert, S.; Demeshko, S.; Reijerse, E. J.; Meyer, F. *Angew. Chem., Int. Ed.* **2015**, *54*, 1738−1743.

(8) Lewis, E. A.; Tolman, W. B. *Chem. Rev.* **2004**, *104*, 1047−1076.

(9) Shiota, Y.; Yoshizawa, K. *Inorg. Chem.* **2009**, *48*, 838−845.

(10) Sirajuddin, S.; Rosenzweig, A. C. *Biochemistry* **2015**, *54*, 2283−2294.

(11) Culpepper, M. A.; Rosenzweig, A. C. *Crit. Rev. Biochem. Mol. Biol.* **2012**, *47*, 483−492.

(12) Halvagar, M. R.; Solntsev, P. V.; Lim, H.; Hedman, B.; Hodgson, K. O.; Solomon, E. I.; Cramer, C. J.; Tolman, W. B. *J. Am. Chem. Soc.* **2014**, *136*, 7269−7272.

(13) Davenport, T. C.; Tilley, T. D. *Angew. Chem., Int. Ed.* **2011**, *50*, 12205−12208.

DOI: 10.1021/acs.inorgchem.6b01504
Inorg. Chem. 2016, 55, 8263−8266

(14) Davenport, T. C.; Tilley, T. D. *Dalton Trans.* **2015**, *44*, 12244−12255.
(15) Farrugia, L. J.; Lovatt, P. A.; Peacock, R. D. *J. Chem. Soc., Dalton Trans.* **1997**, 911−912.
(16) Kodera, M.; Shimakoshi, H.; Tachi, Y.; Katayama, K.; Kano, K. *Chem. Lett.* **1998**, 441−442.
(17) Monzani, E.; Battaini, G.; Perotti, A.; Casella, L.; Gullotti, M.; Santagostini, L.; Nardin, G.; Randaccio, L.; Geremia, S.; Zanello, P.; Opromolla, G. *Inorg. Chem.* **1999**, *38*, 5359−5369.
(18) Lieberman, R. L.; Rosenzweig, A. C. *Nature* **2005**, *434*, 177−182.
(19) Ruiz, E.; Alemany, P.; Alvarez, S.; Cano, J. *Inorg. Chem.* **1997**, *36*, 3683−3688.
(20) Crawford, V. H.; Richardson, H. W.; Wasson, J. R.; Hodgson, D. J.; Hatfield, W. E. *Inorg. Chem.* **1976**, *15* (9), 2107−210.
(21) Zanello, P. *Inorganic electrochemistry: theory, practice and application*, 2nd ed.; Royal Society of Chemistry: Cambridge, U.K., 2003.
(22) Saveant, J.-M. *Elements of molecular and biomolecular electrochemistry: an electrochemical approach in electron transfer chemistry*; Wiley: Hoboken, NJ, 2006.
(23) Bard, A.; Faulkner, L. *Electrochemical Methods: Fundamentals and Applications*; Wiley: Hoboken, NJ, 2000; p 864.
(24) Connelly, N. G.; Geiger, W. E. *Chem. Rev.* **1996**, *96*, 877−910.
(25) The increase of *T* led to a broadening of the signal and a partial decomposition of the complex observable around 150−200K (Figure S15).
(26) Brunschwig, B. S.; Creutz, C.; Sutin, N. *Chem. Soc. Rev.* **2002**, *31*, 168−184.
(27) Winter, R. F. *Organometallics* **2014**, *33*, 4517−4536.
(28) Robin, M. B.; Day, P. *Adv. Inorg. Chem. Radiochem.* **1968**, *10*, 247−422.
(29) The OTf^- in interaction with Cu2, as observed in the solid state, was not taken into account for DFT calculations according to NMR.
(30) Konezny, S. J.; Doherty, M. D.; Luca, O. R.; Crabtree, R. H.; Soloveichik, G. L.; Batista, V. S. *J. Phys. Chem. C* **2012**, *116*, 6349−6356.
(31) Martin, R. L. *J. Chem. Phys.* **2003**, *118*, 4775−4777.

NOTE ADDED AFTER ASAP PUBLICATION

This paper was published on the Web on August 12, 2016, with errors to Table S1 in the Supporting Information. The corrected version was reposted on August 25, 2016.

DOI: 10.1021/acs.inorgchem.6b01504
Inorg. Chem. 2016, 55, 8263−8266